This journal is (c) The Royal Society of Chemistry 2010

1 # Electronic Supplementary Information

2

3 ## Bio-bar-code dendrimer-like DNA as signal amplifier for cancerous
4 ## cells assay using ruthenium nanoparticle-based ultrasensitive
5 ## chemiluminescence detection

6

7 Sai Bi, Shuangyuan Hao, Li Li, and Shusheng Zhang*

8

9 *Key Laboratory of Eco-chemical Engineering, Ministry of Education, College of*
10 *Chemistry and Molecular Engineering, Qingdao University of Science and*
11 *Technology, Qingdao 266042, P. R. China*

12

13

14 *** Corresponding author. Tel.: +86-532-84022750; Fax: +86-532-84022750.**
15 **E-mail: shushzhang@126.com**

1 **Chemicals.** The oligonucleotides sequences (**Table S1**) were commercially synthesized and
2 PAGE purified by SBS Genetech Co. Ltd. (China). $RuCl_3 \cdot 3H_2O$ was purchased from Shanghai
3 Zenith Company (China). A luminol (standard powder, Sigma-Aldrich) stock solution (1.0×10^{-2}
4 M) was prepared by dissolution in 0.1 M NaOH and further stored in dark. The stock solution was
5 consecutively diluted with 0.02 M NaOH-$NaHCO_3$ in order to obtain the proper solution used for
6 FI-CL determination. T4 DNA ligase was ordered from Beijing TransGen Biotech (China).
7 N-hydroxysuccinimide (NHS), 1-ethyl-3-(3-dimethylaminopropyl)-carbodiimide hydrochloride
8 (EDC) were purchased from Sigma. Double-distilled, deionized water was used throughout the
9 experiments. Whole blood samples were provided by Qingdao Papermaking Hospital.

10 **Table S1. DNA Sequences Used in This Work**

Strand	Segment 1	Segment 2
Y_{0a}	5′-TGAC	
Y_{1a}	5′-GTCA	
Y_{2a}	5′-ATCG	TGGATCCGCATGACATTCGCCGTAAG-3’
Y_{3a}	5′-ATGC	
Y_{4a}	5′-GCAA	
Y_{0b}	5′-TGAC	
Y_{1b}	5′-CGAT	
Y_{2b}	5′-GCAT	CTTACGGCGAATGACCGAATCAGCCT-3’
Y_{3b}	5′-TTGC	
Y_{4b}	5′-NH_2-GGAT	
Y_{0c}	5′-TGAC	
Y_{1c}	5′-CGAT	
Y_{2c}	5′-GCAT	AGGCTGATTCGGTTCATGCGGATCCA-3’
Y_{3c}	5′-TTGC	
Y_{4c}	5′-NH_2-GGAT	
Y_{4p}	5′-GAGGAGGGCCAC	
Aptamer	5′-GTGGCCCTCCTCTGGGACTTGTCGGTGGCTTGATAGGAGGGCC ACAAGACAT-NH_2-3’	

11

12 **Apparatus.** The CL detection was conducted on a flow injection chemiluminescence (FI-CL)
13 instrument (MPI-F, Remex Analytical Instrument Co. Ltd., Xi’an, China), including a model

1 IFIS-D flow injection system, a model RFL-1 luminometer, and a computer. The kinetics of CL
2 signals after adding quenchers to luminol-H_2O_2-Ru^{3+} system were investigated on a BPCL
3 ultraweak luminescence analyzer (Institute of Biophysics Academic Sinica, Beijing, China).
4 UV-vis and fluorescence spectra were recorded on a Cary 50 UV-Vis-NIR spectrophotometer
5 (Varian, USA) and a F-4500 fluorescence spectrophotometer (HITACHI, Japan), respectively.
6 Transmission electron microscopy (TEM) and scanning electron microscopy (SEM) images were
7 taken with a H-7650 (HITACHI, Japan) and a JSM-6700F microscope (HITACHI, Japan),
8 respectively.

9 **Preparation of Ruthenium Nanoparticles (RuNPs).** RuNPs were prepared according to the
10 Viau's protocol through the reduction of ruthenium (III) chloride in a liquid polyol. Briefly,
11 $RuCl_3 \cdot 3H_2O$ (0.32 mmol) and sodium acetate (1 mmol) were dissolved in 100 ml of
12 1,2-propanediol. When the temperature was reached at 150 ^{o}C for 10 min with stirring, the color
13 of the solution turned from intense red to pale green and finally to yellowish brown, indicating the
14 reduction and formation of RuNPs. After cooling down the resulting colloidal suspension to room
15 temperature with stirring, the colloidal RuNPs were obtained and separated by centrifugation at 12
16 000 rpm for 30 min. The soft sediment was resuspended in 0.01 M PBS solution and stored at 4 ^{o}C
17 for further use. A UV-vis spectrum was also recorded to confirm the formation of Ru-NPs (**Fig.**
18 **S1A**), and SEM were recorded to confirm the average size of Ru-NPs (**Fig. S1B**).

19 **Construction of Y-DNA and bbc-DL-DNA.** Stock solutions of oligonucleotides were
20 prepared by dissolving in annealing buffer (10 mM Tris-HCl, pH 8.0, 1 mM EDTA, and 50
21 mMNaCl). Taking the construction of Y_0-DNA (shorten as Y_0) as example, the same molar
22 amount of Y_{0a}, Y_{0b} and Y_{0c} were mixed with a final concentration of 5 mM for each

1 oligonucleotide. After denaturing at 95 ^{o}C for 2 min, the solution was quickly cooled down to 60
2 ^{o}C, and further annealing to 4 ^{o}C with a continuous temperature decrease at a ratio of 2 ^{o}C/min.
3 Similarly, Y_1, and Y_n and so on were constructed according to above procedures.
4 For the construction of bbc-DL-DNA, individual Y-DNA was ligated specifically to
5 corresponding Y-DNA. Briefly, 0 generation of DL-DNA (shorten as G_0) was actually the
6 structure of Y_0; G_1 was fabricated by ligating 3 Y_1 with $1G_0$; G_2 was fabricated by ligating 6 Y_2
7 with $1G_1$. Other higher generations of DL-DNA were fabricated in the same way. Note that, for
8 the construction of functionalized G_4, two kinds of Y_4 ($Y_{4a} + Y_{4b} + Y_{4c} \rightarrow Y_4$ and $Y_{4a} + Y_{4b} + Y_{4l}$
9 $\rightarrow Y_4$', l standing for linker DNA, Y_{4b} and Y_{4c} were modified with amino-group) were added at
10 the molar ratio of 23:1 to perform the concept of bio-bar-code DL-DNA (bbc-DL-DNA). For each
11 ligation, the Y-DNA monomer was ligated in ligase buffer containing T4 DNA ligase (200
12 units/μL) at 25 ^{o}C for 1 h.
13 **Agarose Gel Electrophoresis.** Each generation DL-DNA samples were characterized on
14 agarose Ready-Gel. Agarose gel (3%) were prepared in Tris-acetate-EDTA (TAE) buffer (40 mM
15 Tris,20 mM acetic acid and 2 mM EDTA, pH 8.5) and run at 100 V for 30 min. The gel was
16 stained with ethidium bromide (0.5 μg/ ml) in TAE solution. The visualization and photography
17 were performed using a digital camera under UV illumination. The results are shown in **Fig. 1** in
18 the main text.
19 **Fabrication of RuNP-bbc-DL-DNA/aptamer-MBs Conjugates.** A suspension of
20 carboxylated MBs (100 μL) was previously washed with 400 μL of 0.1 M imidazol-HCl buffer
21 (pH 7.0) three times, and activated in a 0.2 M NHS solution (200 μL) and a 0.8 M EDC solution
22 (200 μL) at 37 ^{o}C for 30 min, followed by washing three times with 400 μL of 0.01 M PBS buffer

1 and resuspended to a final volume of 200 μL. And then, 500 μL of 2.0×10^{-8} M amino-modified
2 aptamer was added to ~50 μL of the above resulting MBs solution, and incubated at 37 ^{o}C for 8 h
3 with gentle shaking. Excess aptamers were removed by magnetic force, followed by washing the
4 resulting aptamer-MBs three times with PBS buffer. The RuNP-bbc-DL-DNA/aptamer-MBs
5 conjugates were fabricated by adding 200 μL of G_4 bbc-DL-DNA solution to the above prepared
6 aptamer-MBs and incubated at 37 ^{o}C for 1 h, followed by reacted with Ru-NPs solution (1.0×10^{-4}
7 M) for 12 h. The resulting RuNP-bbc-DL-DNA/aptamer-MBs conjugates were separated from the
8 excess unlabeled Ru-NPs solution magnetically, washed three times with 200 μL of PBS buffer,
9 and resuspended in 200 μL PBS buffer for further use at 4 ^{o}C.
10 **Cancer Cell Culture.** Ramos cells (target cells) and CEM cells (control cells) were cultured in
11 cell flasks separately in RPMI 1640 medium supplemented with 10% (v/v) fetal bovine serum
12 (FBS) and 100 IU/mL penicillin-streptomycin in a humidified atmosphere with 5% CO_2 at 37 ^{o}C.
13 Prior to the experiments, the cell density was counted using a hemocytomer. And then, a 1.0 mL
14 of $\sim 8.0 \times 10^{6}$ cells suspension was centrifuged at 3500 rpm for 5 min and washed five times with
15 phosphate-buffered saline (18.6 mM phosphate, 4.2 mM KCl, and 154.0 mM NaCl). The resulting
16 cells suspension was resuspended in 1.0 mL cell media buffer.
17 **Magnetic Extraction.** After adding 50 μL of RuNP-bbc-DL-DNA/aptamer-MBs conjugates to
18 each cell sample followed by incubating for 15 min at 37 ^{o}C, a magnetic field was employed to
19 separate the supernatant which contained the released RuNP-bbc-DL-DNA probes resulting from
20 the structure-switching of cell aptamers. The amount of released RuNP-bbc-DL-DNA probes were
21 proportional to the amount of target cells and decanted using a pipette for the following FI-CL
22 detection.

1 **FI-CL Detection.** 200 µL of 0.2 M nitric acid solution was used to dissolve RuNPs which were
2 labeled on the released RuNP-bbc-DL-DNA probes. After adjusting the pH of resulting Ru^{3+}
3 solution to 5.0 with NaOH, the volume of the solution was adjusted to 5 mL with 0.02 M HNO_3
4 (pH 5.0). After optimizing the luminol-H_2O_2-Ru^{3+} CL system, the FI-CL detection was performed
5 by mixing 5.0×10^{-4} M luminol in pH 10.0, 0.02 M NaOH-$NaHCO_3$ buffer solution with $4.0 \times$
6 10^{-2} M H_2O_2, and then reacting with metal ions in the flow cell to produce CL signal.

1 **Characterization of Ruthenium Nanoparticles (RuNPs) and Its Assembly on MBs.** The
2 synthesized RuNPs were characterized by UV-vis spectra and SEM images. From **Fig. S1A**, the
3 formation of RuNPs could be confirmed when the UV-vis absorption band at ~400 nm
4 disappeared, indicating that the reduction of Ru^{3+} salt was complete. The size distribution of
5 RuNPs was characterized by SEM images. From **Fig. S1B**, by reduction of $RuCl_3$ in 1,2-propane
6 diol, a mean diameter of 4 nm-sized RuNPs were obtained. In addition, SEM observation of
7 RuNPs prepared by this method exhibited a good dispersion without agglomeration, which further
8 showed an excellent stability against agglomeration since no evident precipitation of metal powder
9 was observed upon standing the colloidal solution at room temperature for one week.

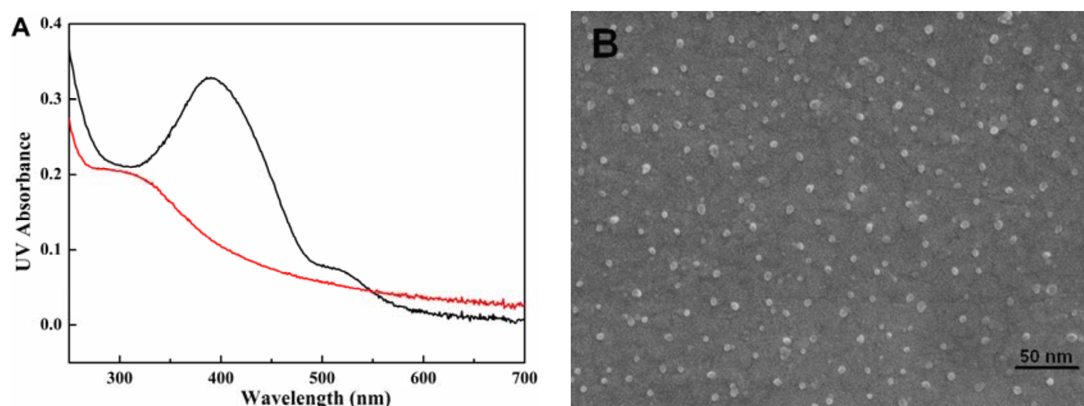

10

11 **Fig. S1.** (A) UV-vis absorption spectra of $RuCl_3$ solution (black curve) and RuNPs (red curve).
12 (B) The SEM images of RuNPs with an average diameter of 4 nm.

13

14 The TEM images of magnetic beads (MBs) before and after conjugation with DL-DNA capped
15 with RuNPs were recorded and shown in **Fig. S2**. The TEM of the construction of
16 RuNP-bbc-DL-DNA/aptamer-MBs conjugates were shown in **Fig. S2B**. Numerous RuNPs could
17 be seen on the surface of the MB compared to that of MB before conjugation as shown in **Fig.**

1 **S2A**. The results indicated that the conjugates of RuNP-bbc-DL-DNA/aptamer-MBs were
2 constructed satisfactorily as expectation.

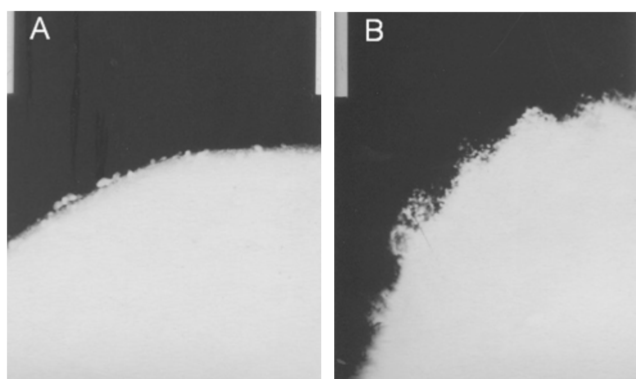

3

4 Fig. S2 The TEM images of magnetic beads (MBs) (A) before and (B) after conjugation with
5 DL-DNA capped with RuNPs.

6

7 Moreover, the amount of RuNPs constructed on the surface of one MB was determined as follows:

8 **Preparation of FI-CL calibration curve of standard RuNPs solutions.** Standard RuNPs
9 solutions were prepared from the solution of 1.0×10^{-3} M RuNPs. The FI-CL calibration curve of
10 RuNPs is shown in **Fig. S3**, the regression equation could be expressed as $Y = -0.0596X^2 +$
11 $17.4568X + 31.3619$ (X is the concentration of RuNPs solution, 10^{-5} M; Y is the FI-CL intensity, n
12 = 12, R = 0.9980).

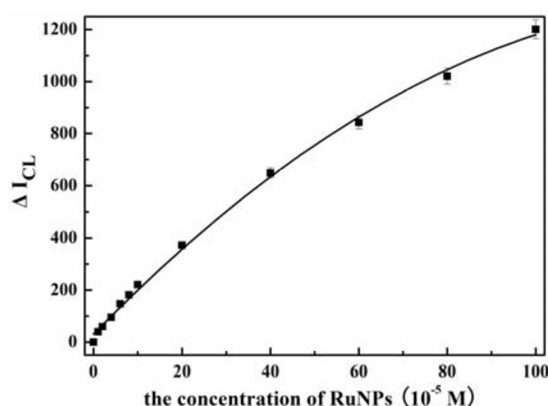

13

14 **Fig. S3** The calibration curve of peak height versus the concentration of RuNPs solution from 1.0
15 $\times 10^{-5}$ to 1.0×10^{-3} M.

1 **Determination of the surface coverages of RuNPs on MBs.** 1.0×10^{-3} M RuNPs solution was
2 reacted with DL-DNA/aptamer-MBs conjugates and incubated for 12 h. Then the supernatant was
3 taken for FI-CL detection. The number of RuNPs immobilized on the MBs can be quantitatively
4 calculated by the FI-CL intensities differences between the RuNPs solution before and after
5 immobilization, which is calculated as below.

6 FI-CL intensity of the background of luminol-H_2O_2 FI-CL system: 63

7 FI-CL intensity of the supernatant before immobilization: 1242

8 → Concentration of RuNPs before immobilization: 9.98×10^{-4} M

9 FI-CL intensity of the supernatant after immobilization: 1027

10 → Concentration of RuNPs after immobilization: 7.04×10^{-4} M

11 Thus, the concentration of RuNPs immobilized on MBs: $(9.98 – 7.04) \times 10^{-4} = 2.94 \times 10^{-4}$ M

12

13 **Calculation of moles of MBs in a given preparation**

14 MNP diameter = 0.75×10^{-4} cm

15 MNP Volume = $4/3\pi r^3 = 1.77 \times 10^{-12}$ cm^3

16 Mass MNP = $\rho_{MNP} \times V_{MNP}$ $=1.18 \times 1.77 \times 10^{-12} = 2.09 \times 10^{-12}$ (g / MNP)

17 The concentration of MNP in 0.01g/mL MNP solution for the preparing

18 $(0.01 \times 10^3) / (2.09 \times 10^{-12}) / (6.02 \times 10^{23}) = 7.95 \times 10^{-12}$ M

19 Thus, $(2.94 \times 10^{-4}) / (7.95 \times 10^{-12}) = 3.7 \times 10^7$ RuNPs were constructed on the surface of one
20 MB.

1 **Optimization of Luminol-H_2O_2-Ru^{3+} FI-CL System.** The effects of luminol and H_2O_2
2 concentrations, and Ru^{3+} standard solution pH in luminol-H_2O_2-Ru^{3+} FI-CL system were
3 investigated comprehensively. As shown in **Fig. S4A**, the signal/background ratios increased with
4 an increase in luminol concentrations from 1.0×10^{-4} to 5.0×10^{-4} mol/L, and decreased with
5 further increasing luminol concentrations. Furthermore, the effect of H_2O_2 concentration on
6 luminol-H_2O_2-Ru^{3+} CL system was studied in the range of $1.0 \times 10^{-3} \sim 1.0 \times 10^{-1}$ mol/L. As shown
7 in **Fig. S4B**, the CL signal/background ratios increased with increasing H_2O_2 concentrations in the
8 range of $1.0 \times 10^{-3} \sim 4.0 \times 10^{-2}$ mol/L, and a maximal signal was obtained at 4.0×10^{-2} mol/L.
9 Therefore, 5.0×10^{-4} mol/L and 4.0×10^{-2} mol/L were selected as the optimal concentrations of
10 luminol and H_2O_2, respectively.

11 As a critical factor of luminol-H_2O_2-Ru^{3+} CL reaction system, the pH value of Ru^{3+} standard
12 solution was studied extensively through adjusting the pH values of Ru^{3+} standard solution in the
13 range of 2.5 to 7.0. From **Fig. S4C**, the maximum CL signal/background ratio was occured at pH
14 5.0 of Ru^{3+} standard solution.

15 After optimizing the conditions of luminol-H_2O_2-Ru^{3+} FI-CL system, the calibration curve of
16 relative CL intenties versus Ru^{3+} concentrations was further investigated. As shown in **Fig. S4D**,
17 the CL intensities were found to increase gradually with increasing the concentration of Ru^{3+}. For
18 the concentrations of 1.0×10^{-8} to 1.0×10^{-6} g/mL Ru^{3+} standard solution, the nonlinear function
19 could be expressed as $I = -0.0708C^2 + 17.7950C + 34.6885$ (I is the relative CL intensity; C is the
20 concentration of Ru^{3+}, 10^{-8} M; $n = 12$, $R^2 = 0.9978$); for the concentrations of 1.0×10^{-8} to $1.0 \times$
21 10^{-7} g/mL Ru^{3+} standard solution, the linear regression equation could be expressed as I =

22.0154C + 13.5034 (C is the concentration of Ru^{3+}, 10^{-8} g/mL; I is relative the CL intensity, n = 7, R = 0.9961).

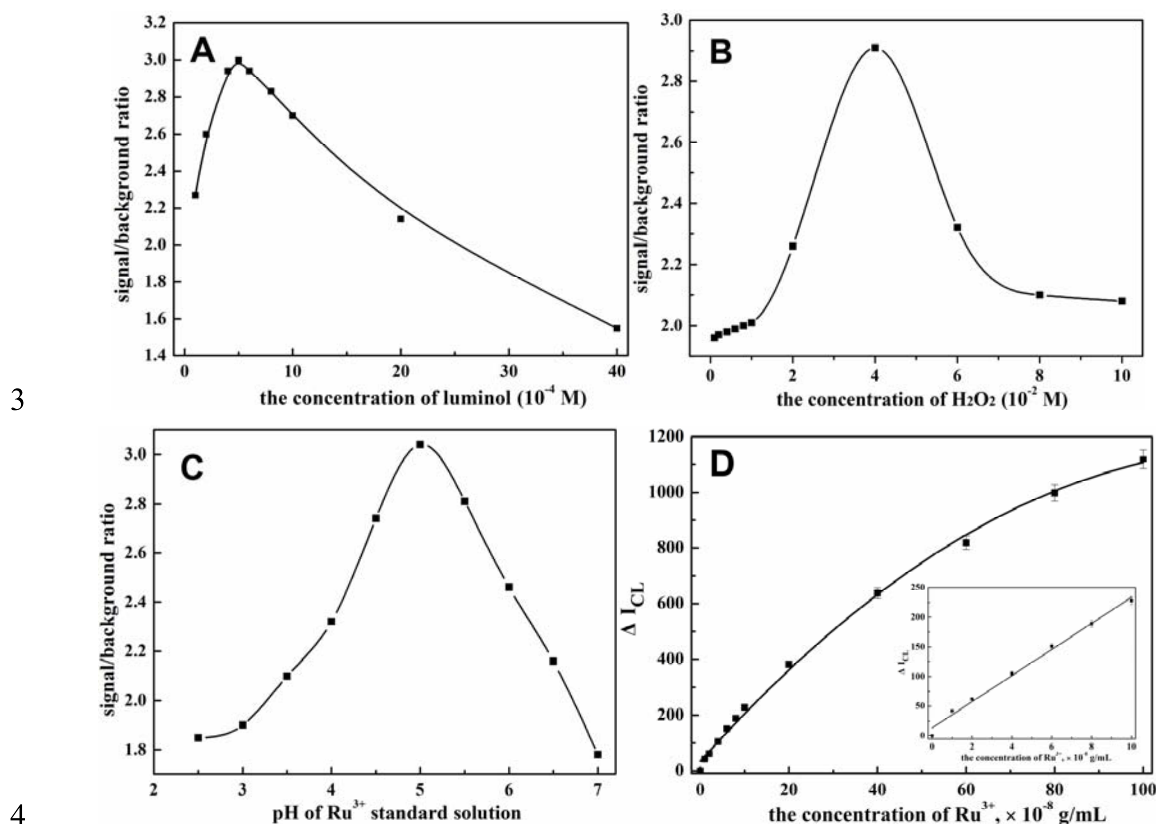

Fig. S4 Effects of the reactant conditions on the luminol-H_2O_2-Ru^{3+} CL system. (A) Effects of the concentration of luminol: pH 10.0, 0.02 M NaOH-$NaHCO_3$ buffer solution, 7.5 × 10^{-3} M H_2O_2 and pH 5.0, 5.0 × 10^{-7} g/mL Ru^{3+} solution. (B) Effects of the concentration of H_2O_2: 5.0 × 10^{-4} M luminol in pH 10.0, 0.02 M NaOH-$NaHCO_3$ buffer solution, pH 5.0, 5.0 × 10^{-7} g/mL Ru^{3+} solution. (C) Effects of Ru^{3+} solution pH: 5.0 × 10^{-4} M luminol in pH 10.0, 0.02 M NaOH-$NaHCO_3$ buffer solution, 4.0 × 10^{-2} M H_2O_2 and 5.0 × 10^{-7} g/mL Ru^{3+} solution. (D) CL signal calibration curve of Ru^{3+} standard solution. The concentration of luminol and H_2O_2 were 5.0 × 10^{-4} M in pH 10.0, 0.02 M NaOH-$NaHCO_3$ buffer solution and 4.0 × 10^{-2} M, respectively. The pH of Ru^{3+} standard solution was 5.0.

1 **Investigation on the Mechanism of Luminol-H_2O_2-Ru^{3+} CL System.**

2
3
4
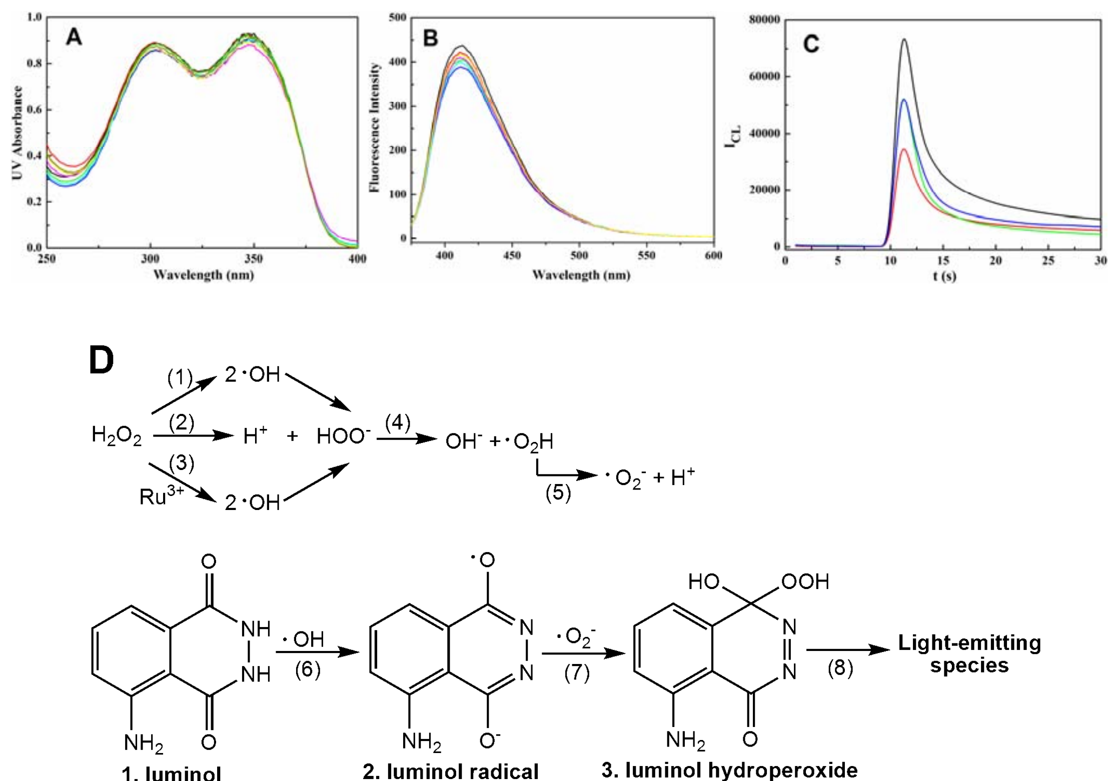

5 **Fig. S5** (A) The UV absorption spectra of luminol (black), luminol-H_2O_2 (red),
6 luminol-H_2O_2-Ru^{3+} (1.0×10^{-6} g/mL, green), luminol-H_2O_2-Ru^{3+} (1.0×10^{-7} g/mL, blue),
7 luminol-H_2O_2-Ru^{3+} (1.0×10^{-8} g/mL, cyan), luminol-Ru^{3+} (1.0×10^{-6} g/mL, magenta),
8 luminol-Ru^{3+} (1.0×10^{-7} g/mL, yellow) luminol-Ru^{3+} (1.0×10^{-8} g/mL, dark yellow). (B)
9 Fluorescence spectra of luminol (black), luminol-Ru^{3+} (1.0×10^{-8} g/mL, red), luminol-Ru^{3+} ($1.0 \times$
10 10^{-7} g/mL, green), luminol-Ru^{3+} (1.0×10^{-6} g/mL, blue), luminol-H_2O_2-Ru^{3+} (1.0×10^{-8} g/mL,
11 cyan) luminol-H_2O_2-Ru^{3+} (1.0×10^{-7} g/mL, magenta) luminol-H_2O_2-Ru^{3+} (1.0×10^{-6} g/mL,
12 yellow). (C) Effect of quenchers on the CL mechanism of luminol-H_2O_2-Ru^{3+} system. Luminol,
13 H_2O_2 and 1.0×10^{-7} g/mL Ru^{3+} were mixed and reacted with H_2O (black), 100 μg/mL SOD (red),
14 0.01 M methyl benzoate (green), and 0.01 M mannitol (blue), respectively. The concentrations of
15 luminol and H_2O_2 were 5.0×10^{-4} M and 4.0×10^{-2} M, respectively. (D) The CL mechanism of
16 luminol-H_2O_2-Ru^{3+} system.

This journal is (c) The Royal Society of Chemistry 2010

1 In order to prove whether the mechanism of luminol-H_2O_2-Ru^{3+} system was the "coordination
2 complex mechanism" or not, the UV-vis and fluorescence spectra were first investigated. From
3 **Fig. S5A and B**, the UV-vis absorption spectra and fluorescence spectra of luminol, luminol-H_2O_2,
4 luminol-Ru^{3+} and luminol-H_2O_2-Ru^{3+} with different Ru^{3+} concentrations seem nearly identical.
5 Thus, it could be proposed that there was no coordination complex formed during the reaction,
6 and the possible CL mechanism of luminol-H_2O_2-Ru^{3+} system was not the "coordination complex
7 mechanism". Consequently, we further investigated the possible CL mechanism of
8 luminol-H_2O_2-Ru^{3+} system by adding different CL quenchers, such as $\cdot O_2^-$ quencher, superoxide
9 dimutase (SOD), and HO· quenchers, mannitol and methanol. From **Fig. S5C** of CL kinetics, the
10 CL intensities were obviously decreased by HO· quenchers, especially quenched by $\cdot O_2^-$ quencher.
11 Thus, it is reasonable that the possible CL mechanism of luminol-H_2O_2-Ru^{3+} system was the "free
12 radical mechanism", which is summerized in **Fig. S5D**.

Control Experiment by Employing Single RuNP as Labels for Assay.

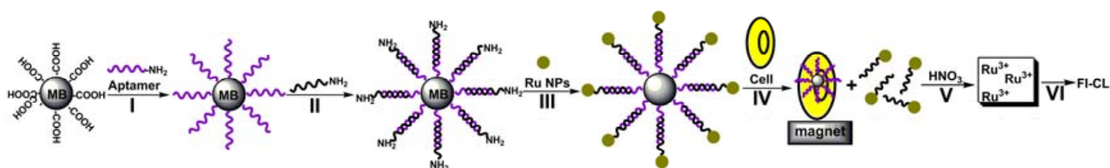

Fig. S6 Schematic illustration of employing single RuNP as labels for the assay of cancer cells based on luminol-H_2O_2-Ru^{3+} FI-CL reaction system.

As controls, we also investigated the assay by employing single RuNP as labels for cancer cells detection (**Fig. S6**). The procedures were performed as described in the main text except using single RuNP rather than bbc-DL-DNA as labels at step (II). As shown in **Fig. S7**, under the optimized experimental conditions, the FI-CL signals of luminol-H_2O_2-Ru^{3+} reaction system increased with the increase of concentrations of Ramos cells ranging from 5000 to 100000 cell/mL with a nonlinear function of $I = -3.4372 \times 10^{-8}C^2 + 0.0117C - 6.0871$ (I is the FI-CL intensity; C is the concentration of target cells, $n = 9$, $R^2 = 0.9991$) and detection limit of 3622 cells/mL, which was ~50-fold higher than that obtained by employing bbc-DL-DNA as labels.

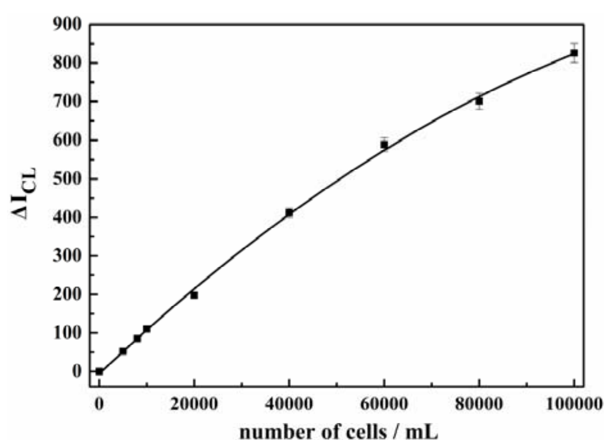

Fig. S7 The calibration curve of peak heights versus the concentrations of target cells from 5000 to 100000 cells/mL.

Investigation of the impact of the DL-DNA capped with RuNPs on the sensitivity of this approach. The impact of the DL-DNA capped with RuNPs on the sensitivity of this approach has been investigated (**Fig. S8**). Upon the introduction of cell samples, bbc-DL-DNA labels (step IVa) and RuNP-bbc-DL-DNA labels (step IVb) were released from the surface of MBs and following dissolved via nitric acid for luminol-H_2O_2 CL system. From the results of our study, the CL intensities obtained from employing bbc-DL-DNA as labels without incubating with RuNPs ($h\upsilon_1$) were approximate to that of luminol-H_2O_2 system ($h\upsilon_0$), while significantly increased by employing RuNPs-bbc-DL-DNA as labels ($h\upsilon_2$). The concentration of target cells for each assay was 1000 cells/mL. Thus, it could be deduced that the DL-DNA has no influence on the sensitivity of this approach, which could ascribe to the denaturation of DNA dendrimers under the strong acid conditions at step V in order to dissolve RuNPs into Ru^{3+} ions for FI-CL detection.

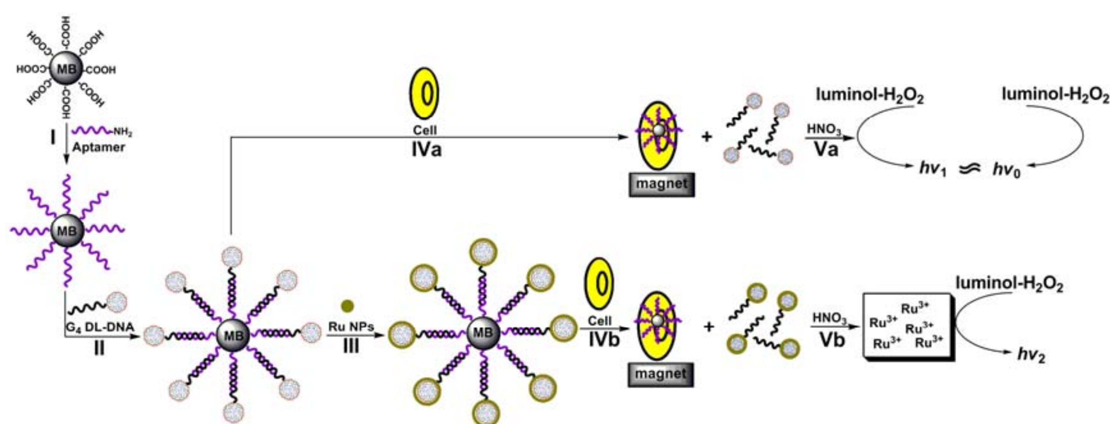

Fig. 8 Investigation of the impact of the DL-DNA capped with RuNPs on the sensitivity of this approach.

This journal is (c) The Royal Society of Chemistry 2010

1 **Mixed Cell Samples Assay.**

2

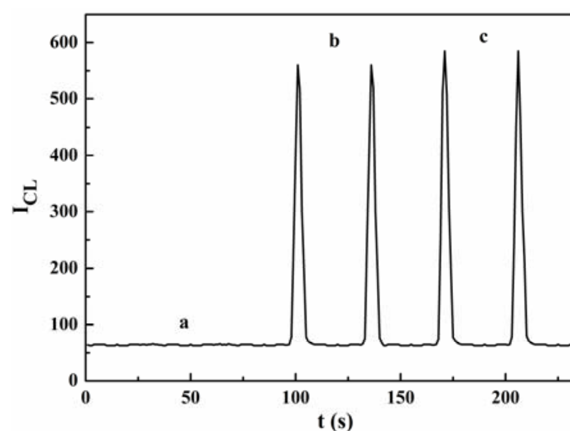

3

4 **Fig. S9** FI-CL signals of (a) blank sample, (b) pure Romas target cells sample, and (c) Romas

5 target cells and CEM control cells mixing sample. Both concentrations of target cells and control

6 cells are 2000 cells/mL.

7

8 **Table S2.** FI-CL Signals of Blood Samples Spiked with and without Romas Target Cells

Sample	Blood sample (cells/mL)	Added target cells (cells/mL)	Detected cells (cells/mL)	Recovery (%)
1	- [a]	100	62	62.0
2	-	1000	713	71.3
3	-	10000	8652	86.5

9 [a] No FI-CL response